Pre-existing virus-specific CD8$^+$ T-cells provide protection against pneumovirus-induced disease in mice

Mary J. G. van Helden[a], Peter J. S. van Kooten[a], Cornelis P. J. Bekker[a], Andrea Gröne[b], David J. Topham[c], Andrew J. Easton[c], Claire J. P. Boog[d], Dirk H. Busch[e], Dietmar M. W. Zaiss[a], and Alice J. A. M. Sijts[a]

[a]Division of Immunology, Faculty of Veterinary Medicine, University of Utrecht, Yalelaan 1, 3571 EK Utrecht, The Netherlands; [b]Division of Pathology, Faculty of Veterinary Medicine, University of Utrecht, Yalelaan 1, 3571 EK Utrecht, The Netherlands; [c]D. Smith Center for Vaccine Biology and Immunology, University of Rochester Medical Center, 601 Elmwood Avenue, Rochester, NY 14642, USA; [d]School of Life Sciences, Gibbet Hill Campus, University of Warwick, Coventry CV4 7AL, UK; [e]Department of Vaccinology, Centre for Infectious Disease Control, National Institute for Public Health and the Environment (RIVM), Antonie van Leeuwenhoeklaan 9, 3721 MA Bilthoven, The Netherlands; [f]Institute for Medical Microbiology, Immunology and Hygiene, Technische Universität München, Trogerstrasse 30, 81675 München, Germany.

Correspondence to: Dr. Alice J.A.M. Sijts or Dr. D. Zaiss, Division of Immunology, Faculty of Veterinary Medicine, University of Utrecht, Yalelaan 1, 3584 CL Utrecht, The Netherlands, Phone: +31302532471, Fax: +31302533555, e-mail: e.j.a.m.sijts@uu.nl or d.zaiss@uu.nl

ABSTRACT

Pneumoviruses such as pneumonia virus of mice (PVM), bovine respiratory syncytial virus (bRSV) or human (h)RSV are closely related pneumoviruses that cause severe respiratory disease in their respective hosts. It is well-known that T-cell responses are essential in pneumovirus clearance, but pneumovirus-specific T-cell responses also are important mediators of severe immunopathology. In this study we determined whether memory – or pre-existing, transferred virus-specific $CD8^+$ T-cells provide protection against PVM-induced disease. We show that during infection with a sublethal dose of PVM, both natural killer (NK) cells and $CD8^+$ T-cells expand relatively late. Induction of $CD8^+$ T-cell memory against a single $CD8^+$ T- cell epitope, by dendritic cell (DC)-peptide immunization, leads to partial protection against PVM challenge and prevents Th2 differentiation of PVM-induced CD4 T-cells. In addition, adoptively transferred PVM-specific $CD8^+$ T-cells, covering the entire PVM-specific $CD8^+$ T-cell repertoire, provide partial protection from PVM-induced disease. From these data we infer that antigen-specific memory $CD8^+$ T-cells offer significant protection to PVM-induced disease. Thus, $CD8^+$ T-cells, despite being a major cause of PVM-associated pathology during primary infection, may offer promising targets of a protective pneumovirus vaccine.

Key words: Pneumoviruses; pneunomia virus of mice; NK cell; $CD8^+$ T-cell; vaccine

Footnote

Abbreviations: BAL, bronchoalveolar lavage; BALF, BAL fluid; DC, dendritic cell; BM-DC, bone marrow derived DC; DCp, peptide-loaded DC; FI, formalin inactivated; hRSV, human respiratory syncytial virus; ID, infectious dose; EID, egg ID; i.n., intranasal; i.p., intraperitoneal; i.v., intravenous; MLN, mediastinal lymph node; NK, natural killer; NS, nonstructural; p.i., post infection; pfu, plaque forming units; PVM, pneunomia virus of mice; SEM, standard error of mean.

1. Introduction

Pneumoviruses are an important cause of respiratory infections in mammals [1]. One well-known member of the pneumovirus genus is hRSV, a major cause of severe respiratory disease in infants and elderly [2]. A failed vaccine trial using formalin-inactivated hRSV (FI-RSV) in the 1960s that led to enhanced disease instead of immune protection [3-6], has triggered intense efforts to elucidate how to induce immune responses that can prevent or protect against natural hRSV infection without causing pathology. Different studies in humans and mouse models have shown that antibodies can contribute to immune protection [7-10]. However, the antibodies induced during natural hRSV infection fail to prevent recurrent infections throughout life, indicating that also the efficacy of vaccine-induced neutralizing antibodies may be limited [7,11]. Controversy also exists concerning the precise role of the T cell compartment in pneumovirus-induced disease [12,13]. Several studies have shown that although T cells are essential in eradicating established infections [14], they also are important mediators of hRSV-induced immunopathology [15-19]. In murine models, especially Th2 skewing of the $CD4^+$ T-cell lineage after immunization with FI-RSV or hRSV-G protein encoding recombinant Vaccinia Virus vectors have been shown to lead to enhanced disease following subsequent hRSV infection [12,13,20]. Induction of $CD8^+$ T-cell responses, on the other hand, inhibited vaccine-enhanced pulmonary disease [21-23]. Thus, despite the notion that T cells play a role in pneumovirus-induced immunopathology, these studies suggest that vaccines designed to induce antipneumoviral $CD8^+$ T cell responses may offer an alternative to vaccines targeting the humoral response.

Pneumoviruses display a narrow host range and several species-specific variants have been described [1], adapted for evasion of defense mechanisms in

their specific hosts [24,25]. Therefore, instead of hRSV, its mouse-adapted variant PVM is increasingly used to study pneumovirus-specific immune responses and immunopathogenesis in mouse models. PVM and hRSV display a marked genetic similarity and use similar evasion strategies [26-28]. Intranasal (*i.n.*) administration of a low PVM inoculum results in effective replication and severe respiratory disease in mice, with several hallmarks similar to severe hRSV disease in humans, including severe pulmonary inflammation, edema, and influx of granulocytes [29].

Although extensively studied during hRSV infections in mouse models, only limited studies evaluated T cells in PVM infected mice [30,31]. Frey et al showed that, like in hRSV-infection, T-cells are essential for viral elimination in PVM-infected mice, but are also important mediators of infection-associated pathology. This observation raises the question of whether a pneumovirus-vaccine that targets $CD8^+$ T cell responses would be safe. In this study, we used the PVM mouse model of respiratory infection to determine whether pre-existing virus-specific $CD8^+$ T-cells may provide protection against pneumovius-induced disease.

2. Material and methods

2.1. Virus stocks, mice and infection

PVM strain J3666 was passaged in mice to retain full pathogenicity and hRSV strain A2 was grown in BSC-1 cells and concentrated as described [32]. For both viruses, plaque assays on BSC-1 cells were performed to determine viral titers. Influenza strains A/HK/x31 (H3N2) and A/PR/8/34 (H1N1) were grown as

described [33]. Age-matched 7-10 week old female BALB/c mice were purchased from Charles River, anesthetized with isoflurane and then infected *i.n.* with $5x10^6$ pfu RSV in 50 μl, or with $1x10^5$ EID_{50} HKx31 or 150 EID_{50} PR8 in 30 μl PBS as described [33], or with the indicated doses of PVM in 30 μl PBS. All animal experiments were approved by the Committee on Animal Experiments of the University of Utrecht.

2.2. Sample preparation

Mice were sacrificed by injection of sodium pentobarbital and bronchoalveolar lavage (BAL) was collected by three times lavage with 1 ml PBS containing 10 μM EDTA. Thereafter, lungs were perfused with PBS, excised, minced and incubated in PBS containing collagenase (2.4 mg/ml; Roche Applied Science) and DNase (1 mg/ml; Roche Applied Science) for 30 minutes at 37°C, passed through a cell strainer and lymphocytes were purified using lympholyte-M (Cederlane). For mRNA isolation, the right lung was placed in 1 ml TRIzol (Invitrogen).

2.3. Flow cytometry

Fluorochrome-conjugated antibodies were purchased from eBioscience [CD69 (H1.2F3), CD49b (DX5), TCRβ (H57-597), NKp46 (29A1.4), CD62L (MEL-14), IFNy (XMG1.2), CD8 (53-6.7), CD11c (N418), CD19 (MB19-1), CD4 (RM4-5), MHC-II (m5/114.15.2)] or BD Pharmingen [Siglec-F (E50-2440)]. PE-labeled MHC class I tetramers were prepared in collaboration with D. Busch (TU-Muenchen), by refolding H2-K^d heavy chains and human β_2m in the presence of synthetic influenza-derived $NP_{147-155}$ (TYQRTRALV), hRSV $M2_{82-90}$ (SYIGSINNI) or PVM

$P_{261-269}$ (CYLTDRARI). Cell surface markers were stained as described [34]. For tetramer stainings, cells were incubated with 1 μg tetramer for 1 hour at 4 ^{0}C and then stained for surface markers. To measure IFNγ production, BAL cells were stimulated 1:1 with YAC cells for 4 hours (NK cell activation) or with 2 μM $P_{261-269}$ for 6 hours ($CD8^+$ T-cell stimulation) in 100 μl RPMI medium containing 10% FCS, glutamax, antibiotics and 30 μM β-mercaptoethanol, and 10 μM monensin and then stained as described [34]. Cells were analyzed on a FACS Calibur or Canto II (BD Biosciences) using FlowJo software (Tree Star).

2.4. Preparation of peptide-loaded bone marrow (BM)-DC and FI-PVM

Mouse BM-DC were expanded for 6 days in RPMI medium with 15% GM-CSF (culture supernatant of X63Ag cells), activated overnight with 100 ng/ml LPS and then pulsed for 1 hour with 2 μM $P_{261-269}$. Mice were immunized intravenously (*i.v.*) with 5 x 10^6 peptide-loaded BM-DC in 200 μl PBS. FI-PVM was prepared as described [6] and was administered in 100 μl *s.c.* Mice were infected with PVM, 3-5 weeks after immunization.

2.5. Quantitative real-time PCR

Total lung RNA was purified using TRIzol (Invitrogen) and cDNA was transcribed (iScript cDNA Synthesis Kit; Bio-Rad Laboratories). PVM_{SH} RT-PCR was performed as described [35] in an iCycler (Bio-Rad Laboratories), 95 °C for 10 min and then 45 cycles of 95 °C for 15s and 60 °C for 60s. Copy numbers per lung were calculated from a standard curve generated using serially diluted PVM-SH cDNA. RT-PCR for IL-4, IFNγ and GAPDH were performed using the TaqMan Gene Expression Assays (Applied Biosystems) Mm00445259, Mm00801778 and

Mm99999915. Relative expression of IL-4 and IFNγ normalized against GAPDH were calculated using a fixed point of the standard curve as calibrator.

2.6. Multiplex bead-based assay

To quantify IL-4 and IFNγ, fluoresceinated microbeads coated with capture antibodies (IL-4: BVD-1D11; IFN-γ:AN-18) were added to 50 µl BAL fluid and incubated overnight at 4 °C. Cytokines were detected with biotinylated anti-IFNγ (XMG1.2) and -IL-4 (BVD6-24G2), and PE-labeled streptavidin. Fluorescence was measured using a Luminex model 100 XYP (Luminex, Austin, TX, USA). Antibodies were purchased from BD Biosciences.

2.7. Adoptive transfer of $CD8^+$ T-cells

Naïve and PVM-infected (d. 14 p.i.) donor mice were sacrificed, single cell suspensions prepared of lungs, spleens and MLNs were mixed and stained with PE-labeled antibodies against CD19, CD4, MHC-II and NKp46 (without Fc-block). Negative selection was performed using a BD Influx (BD Biosciences). Recipient mice received 5 x 10^6 enriched cells in 200 µl PBS *i.v.*, and then were infected with PVM.

3. Results

3.1. Dynamics of $CD8^+$ T-cell responses in PVM-infected mice

I.n. infection with 25 pfu of PVM strain J3666 induced severe but sublethal disease in BALB/c mice, with weight reduction of approximately 15 - 20% of original body weight (data not shown). During the first days of infection, PVM

188 rapidly replicated to high numbers (Fig. 1A). Viral copy numbers peaked at d. 8
189 p.i. and then declined.
190 In order to determine their protective capacity, we first studied $CD8^+$ T-cell
191 kinetics during primary PVM infection and compared these with the well-described
192 $CD8^+$ T- cell responses in influenza and hRSV-infected mice [36, 37]. The relative
193 proportions of $CD8^+$ T-cells in the airways of PVM-infected mice strongly
194 increased over time (Fig. 1B), and from d. 10 onwards approximately 60% of
195 lymphocytes in the BAL were $CD8^+$ T-cells. In influenza- and hRSV-infected mice,
196 initially, the proportions of $CD8^+$ T-cells in the airways were higher than in PVM-
197 infected mice but then dropped, when relative proportions of $CD8^+$ T-cells in PVM-
198 infected mice were still rising (Fig. 1B). Quantification of virus-specific $CD8^+$ T-
199 cells with MHC class I tetramers containing a dominant epitope of either PVM
200 ($P_{261-269}$ [30]), influenza ($NP_{147-155}$ [38]) or hRSV ($M2_{82-90}$ [39]), demonstrated that
201 $NP_{147-155}$- and $M2_{82-90}$-specific $CD8^+$ T-cells were detectable at d. 6 p.i. and
202 expanded until d. 8-10 p.i. when a plateau was reached (Fig. 1C). In PVM-infected
203 mice, the BAL did not contain any $P_{261-269}$-specific $CD8^+$ T-cells at d. 6 p.i, and only
204 a small population of $P_{261-269}$-specific $CD8^+$ T-cells could be detected at d. 8 p.i.
205 (Fig. 1D, E). The relative proportions of $P_{261-269}$ $tetramer^+$ $CD8^+$ T-cells further
206 increased until d. 10 p.i. after which levels remained high (Fig. 1D, E). To
207 determine whether PVM -specific $CD8^+$ T-cell were functional, we quantified IFNγ
208 production in virus-specific $CD8^+$ T-cells after *ex vivo* $P_{261-269}$ stimulation.
209 Consistent with earlier publications [30,37], we found that IFNγ producing $P_{261-269}$-
210 specific $CD8^+$ T-cells were barely detectable at d. 8 of infection (Fig. 1F, G) but
211 then increased in numbers. At any time point of infection, the relative proportions
212 of IFNγ-producing $P_{261-269}$-specific $CD8^+$ T-cells remained lower than that of $P_{261-269}$
213 tetramer-stained cells. From these data we conclude that high proportions of $CD8^+$

T-cells migrate to the lungs of PVM infected mice and that the appearance of virus-specific $CD8^+$ T-cells in the airways is slightly delayed compared to influenza virus- or hRSV-infected mice.

3.2. Dynamics of innate responses to PVM infection

As PVM-specific $CD8^+$ T-cells migrated relatively late to the lungs of PVM infected mice, we wondered whether migration of other immune cells was delayed also. Quantification of NK cells in the BAL demonstrated a prominent influx of NK cells into the airways of PVM-infected mice at d. 6 of infection, when approximately 50% of total infiltrating lymphocytes were NK cells (Fig. 2A, left panel). In absolute numbers (Fig. 1A, right panel) NK cell responses in PVM-infected mice peaked between days 8 and 10 of infection and then declined. In comparison, in the airways of influenza strain HKx31-infected mice (Fig. 1A) a large influx of NK cells, representing approximately 60% of total lymphocytes, was detected already at d. 2 p.i. with absolute numbers of infiltrating NK cells peaking at d. 3 of infection. Similar results were obtained in analyses of the BAL of hRSV-infected mice (Supplemenary Fig. 1). Both in influenza- and in PVM-infected mice, BAL NK cells displayed an activated phenotype (high CD69) and produced IFNγ upon stimulation *ex vivo* (Fig. 2B, C), indicating that they were functional. Thus, PVM-infected mice show a marked influx of NK cells into the airways, although at a later time point than in mice infected with influenza or hRSV.

PVM is a natural mouse pathogen and, unlike in case of HKx31, only a few viral particles suffice to establish severe disease in mice. To determine whether the low numbers of infecting virus particles explains for the shifted kinetics of NK cell responses in PVM compared to HKx31-infected mice, NK cell influx into the airways of PVM-infected mice was compared to that in mice infected with the

mouse-adapted influenza strain PR8, which is more virulent than HKx31 and therefore used at 100-1000 fold lower concentration. Still, like HKx31, infection with PR8 (150 EID_{50}) induced a prominent early NK cell influx into the airways (Fig. 2D, d. 2 and 4 p.i). Conversely, mice infected with a high dose of PVM (1250 pfu) lacked NK cells in the BAL at d. 2 p.i., and only minor numbers of NK cells were detected at d. 4 p.i. (Fig. 2D). In conclusion, both $CD8^+$ T-cells and NK cells migrate to the BAL at a much later time point following infection with PVM than with influenza. The relatively late influx of NK cells into the airways of PVM-infected mice is likely to be explained by specific properties of this pneumovirus rather than by the low numbers of viral particles administered to cause infection.

3.3. $P_{261-269}$-specific memory $CD8^+$ T-cells provide partial protection against PVM-induced disease

It has been shown that in PVM-infected mice, T-cells are responsible for viral clearance, but are also involved in immunopathology [31]. To determine whether PVM-specific memory $CD8^+$ T-cells may confer immune protection, mice were immunized with GM-CSF-expanded BM-DC loaded with synthetic $P_{261-269}$ (DCp) and then challenged with PVM. As shown in Figs 3A and 3B, numbers of $P_{261-269}$-specific $CD8^+$ T-cells detected in the BAL of immunized mice were substantially higher than in non-immunized controls (Fig. 3A, B). Over the duration of the infection, DCp-primed mice lost less weight (Fig. 3C), displayed significantly reduced total-cell influx in the BAL (Fig. 3D), viral loads were significantly lower than in non-immunized mice (Fig. 3E), and peribronchial and interstitial cellular infiltrates were reduced (Supplementary Fig. 2), indicating an enhanced control of disease and viral loads.

Since vaccination with FI-PVM elicits an enhanced Th2 response upon PVM infection [40], we investigated the effect of DCp immunization on CD4 T-cell differentiation during PVM challenge. Compared with FI-PVM-immunized controls, mice immunized with $P_{261-269}$-loaded DC displayed elevated amounts of IFNγ mRNA and cytokine levels in the lungs following challenge, indicating that they had developed a Th1-skewed immune response (Fig. 4A, B; upper panels). In contrast, FI-PVM immunized mice developed a Th2-skewed response, as indicated by the relatively high levels of IL-4 in the lungs (Fig. 4A, B; lower panels) and eosinophilia in two out of four mice (Fig. 4C, D). Thus, the presence of memory $CD8^+$ T-cells specific for a single PVM-epitope led to enhanced control of virus replication and prevented Th2 skewing of PVM-induced CD4 T-cell responses upon PVM challenge, leading to a reduction of PVM-induced disease.

3.4. Protection conferred by adoptively transferred PVM-specific $CD8^+$ T-cells

Since immunization with $P_{261-269}$-loaded DC provided partial protection, we decided to assess the protective capacity of the total PVM-specific $CD8^+$ T-cell response, targeting multiple epitopes. A mix of $CD8^+$ T-cells enriched from the spleen, MLN and lungs of PVM-infected or uninfected mice were adoptively transferred into recipient mice that then were infected with PVM. At d. 7 p.i. a clear population of $P_{261-269}$-$tetramer^+$ cells was detectable in the lungs of mice that had received $CD8^+$ T-cells of PVM-infected donors, but not in the lungs of recipients that had received naïve $CD8^+$ T-cells of uninfected controls (Fig. 5A, B). In addition, recipients receiving immune cells from infected mice showed significantly reduced weight-loss and viral load (Fig. 5C, D). These results show that PVM-specific $CD8^+$ T-cells, despite being a major cause of pathology in pneumovirus infections, can provide protection against PVM infection.

4. Discussion

Despite the fact that hRSV is a major cause of disease in infants, there still are major gaps in our knowledge of the host response against this virus. There is an increasing interest in using the natural mouse pathogen PVM to mimic and study severe pneumovirus infections. We have used this model to study the role of $CD8^+$ T-cells in conferring protection against disease. Influx of both NK and $CD8^+$ T-cells into the BAL of PVM-infected mice was markedly delayed compared to that in mice infected with influenza or hRSV (Fig. 1, 2). However, from d. 10 p.i. onwards, extremely high numbers of $CD8^+$ T-cells were present in the airways of PVM-infected mice, coinciding with disease. The relatively late immune activation seen in the PVM-infected mice was not explained by the quantities of administered viral particles, as both sublethal and lethal doses of PVM failed to induce an early NK cell influx in the infected respiratory tissue (Fig. 1), whereas both high dose HKx31 and low dose PR8 (representing comparable ID50s) caused an early NK cell influx, well detectable at d. 2 p.i. If not the quantities of administered particles, differing replication kinetics may explain the differences in kinetics of immune activation between PVM and influenza infection, although it should be noted that PVM rapidly replicates during the first days of infection, reaching titers of approximately 10^5 particles/lung at d.2 p.i. (Fig. 1) . Alternatively, the relatively late influx of lymphocytes into the airways of PVM-infected mice is consistent also with recent observations that the nonstructural proteins of PVM (NS1 and NS2) inhibit type I and type III interferon responses [27,28]. In these studies, inflammation in the airways of PVM-infected mice was found to be still limited at d. 3 p.i., while at d. 6 p.i., high levels of chemokines and cytokines such as MCP-1, RANTES, MIP-1α and IL-15 were produced [27,28]. These

316 chemokines are likely to attract NK cells to the airways, as well as $CD8^+$ T-cells
317 [31].
318 The finding that $CD8^+$ T-cells cause pathology in the PVM-mouse model
319 [31] has raised questions about the use of a vaccine designed to stimulate a
320 pneumovirus-specific $CD8^+$ T-cell response. However, we show that mice
321 immunized with BM-DCs pulsed with PVM $P_{261-269}$ displayed a Th1-skewed
322 immune response and reduced viral loads following challenge (Fig. 3 and 4),
323 suggesting that vaccine-induced $CD8^+$ T-cell memory protects against
324 pneumovirus-induced disease. In an earlier study [41], immunization with PVM
325 $P_{261-269}$ in IFA was unsuccessful in protecting mice against PVM-infection unless
326 co-administered with a PVM-derived CD4 T-cell epitope. Interestingly, the
327 peptide/IFA immunization protocol used in that study resulted in mixed Th1/Th2
328 responses to the included CD4 T-cell epitope, in contrast to the Th1 responses
329 observed in PVM-challenged DCp-immunized mice (Fig. 3). Thus, immunization-
330 induced PVM-specific memory $CD8^+$ T-cells protect against PVM-associated
331 disease, but the degree of protection and effects of immunization on CD4 T-cell
332 differentiation depend on the strategy for epitope delivery and used adjuvant.
333 Importantly, transfer of $CD8^+$ T-cells isolated from PVM-infected mice, which are
334 targeted to a broad range of epitopes, almost entirely abrogated weight-loss in
335 recipients and significantly reduced viral loads following challenge with PVM (Fig.
336 5). Taken together, the data presented here demonstrate that the presence of
337 already primed PVM-specific $CD8^+$ T-cells at the time point of PVM-infection leads
338 to enhanced control of viral loads and prevents T-cell-driven immunopathology.
339 In conclusion, we have shown PVM-specific $CD8^+$ T-cells provide partial
340 protection against PVM-induced disease, probably by preventing Th2 skewing of
341 PVM-specific immune responses and by early control of viral loads. Our findings

strongly suggest that pneumovirus vaccines designed to induce antigen-specific $CD8^+$ T-cell memory may offer effective protection against pneumovirus-induced disease.

Acknowledgements

Funding: This work was supported by Top Institute Pharma [T4-214]; and the Wellcome Trust [WT 085733MA].

References

[1] Easton AJ, Domachowske JB, Rosenberg HF. Animal pneumoviruses: molecular genetics and pathogenesis. Clin Microbiol Rev 2004;17(2):390-412.

[2] Thompson WW, Shay DK, Weintraub E, Brammer L, Cox N, Anderson LJ et al. Mortality associated with influenza and respiratory syncytial virus in the United States. JAMA 2003;289(2):179-86.

[3] Chin J, Magoffin RL, Shearer LA, Schieble JH, Lennette EH. Field evaluation of a respiratory syncytial virus vaccine and a trivalent parainfluenza virus vaccine in a pediatric population. Am J Epidemiol 1969;89(4):449-63.

[4] Fulginiti VA, Eller JJ, Sieber OF, Joyner JW, Minamitani M, Meiklejohn G. Respiratory virus immunization. I. A field trial of two inactivated respiratory virus vaccines; an aqueous trivalent parainfluenza virus vaccine and an alum-precipitated respiratory syncytial virus vaccine. Am J Epidemiol 1969;89(4):435-48.

[5] Kapikian AZ, Mitchell RH, Chanock RM, Shvedoff RA, Stewart CE. An epidemiologic study of altered clinical reactivity to respiratory syncytial (RS) virus infection in children previously vaccinated with an inactivated RS virus vaccine. Am J Epidemiol 1969;89(4):405-21.

[6] Kim HW, Canchola JG, Brandt CD, Pyles G, Chanock RM, Jensen K et al. Respiratory syncytial virus disease in infants despite prior administration of antigenic inactivated vaccine. Am J Epidemiol 1969;89(4):422-34.

[7] Hall CB, Walsh EE, Long CE, Schnabel KC. Immunity to and frequency of reinfection with respiratory syncytial virus. J Infect Dis 1991;163(4):693-8.

[8] Piedra PA, Jewell AM, Cron SG, Atmar RL, Glezen WP. Correlates of immunity to respiratory syncytial virus (RSV) associated-hospitalization: establishment of minimum protective threshold levels of serum neutralizing antibodies. Vaccine 2003;21(24):3479-82.

[9] Falsey AR, Walsh EE. Relationship of serum antibody to risk of respiratory syncytial virus infection in elderly adults. J Infect Dis 1998;177(2):463-6.

[10] Fenton C, Scott LJ, Plosker GL. Palivizumab: a review of its use as prophylaxis for serious respiratory syncytial virus infection. Paediatr Drugs 2004;6(3):177-97.

[11] Henderson FW, Collier AM, Clyde WA,Jr, Denny FW. Respiratory-syncytial-virus infections, reinfections and immunity. A prospective, longitudinal study in young children. N Engl J Med 1979;300(10):530-4.

386 [12] Braciale TJ. Respiratory syncytial virus and T cells: interplay between the
387 virus and the host adaptive immune system. Proc Am Thorac Soc 2005;2(2):141-
388 6.

389 [13] Castilow EM, Olson MR, Varga SM. Understanding respiratory syncytial virus
390 (RSV) vaccine-enhanced disease. Immunol Res 2007;39(1-3):225-39.

391 [14] Ostler T, Ehl S. Pulmonary T cells induced by respiratory syncytial virus are
392 functional and can make an important contribution to long-lived protective
393 immunity. Eur J Immunol 2002;32(9):2562-9.

394 [15] Ostler T, Davidson W, Ehl S. Virus clearance and immunopathology by
395 CD8(+) T cells during infection with respiratory syncytial virus are mediated by
396 IFN-gamma. Eur J Immunol 2002;32(8):2117-23.

397 [16] Alwan WH, Record FM, Openshaw PJ. CD4+ T cells clear virus but augment
398 disease in mice infected with respiratory syncytial virus. Comparison with the
399 effects of CD8+ T cells. Clin Exp Immunol 1992;88(3):527-36.

400 [17] Cannon MJ, Openshaw PJ, Askonas BA. Cytotoxic T cells clear virus but
401 augment lung pathology in mice infected with respiratory syncytial virus. J Exp
402 Med 1988;168(3):1163-8.

403 [18] Graham BS, Bunton LA, Wright PF, Karzon DT. Role of T lymphocyte subsets
404 in the pathogenesis of primary infection and rechallenge with respiratory syncytial
405 virus in mice. J Clin Invest 1991;88(3):1026-33.

406 [19] Tregoning JS, Yamaguchi Y, Harker J, Wang B, Openshaw PJ. The role of T
407 cells in the enhancement of respiratory syncytial virus infection severity during
408 adult reinfection of neonatally sensitized mice. J Virol 2008;82(8):4115-24.

409 [20] Varga SM, Braciale TJ. RSV-induced immunopathology: dynamic interplay
410 between the virus and host immune response. Virology 2002;295(2):203-7.

411 [21] Hussell T, Baldwin CJ, O'Garra A, Openshaw PJ. CD8+ T cells control Th2-
412 driven pathology during pulmonary respiratory syncytial virus infection. Eur J
413 Immunol 1997;27(12):3341-9.

414 [22] Stevens WW, Sun J, Castillo JP, Braciale TJ. Pulmonary eosinophilia is
415 attenuated by early responding CD8(+) memory T cells in a murine model of RSV
416 vaccine-enhanced disease. Viral Immunol 2009;22(4):243-51.

417 [23] Srikiatkhachorn A, Braciale TJ. Virus-specific CD8+ T lymphocytes
418 downregulate T helper cell type 2 cytokine secretion and pulmonary eosinophilia
419 during experimental murine respiratory syncytial virus infection. J Exp Med
420 1997;186(3):421-32.

421 [24] Bossert B, Conzelmann KK. Respiratory syncytial virus (RSV) nonstructural
422 (NS) proteins as host range determinants: a chimeric bovine RSV with NS genes
423 from human RSV is attenuated in interferon-competent bovine cells. J Virol
424 2002;76(9):4287-93.

425 [25] Lo MS, Brazas RM, Holtzman MJ. Respiratory syncytial virus nonstructural
426 proteins NS1 and NS2 mediate inhibition of Stat2 expression and alpha/beta
427 interferon responsiveness. J Virol 2005;79(14):9315-9.

428 [26] Rosenberg HF, Bonville CA, Easton AJ, Domachowske JB. The pneumonia
429 virus of mice infection model for severe respiratory syncytial virus infection:
430 identifying novel targets for therapeutic intervention. Pharmacol Ther
431 2005;105(1):1-6.

432 [27] Buchholz UJ, Ward JM, Lamirande EW, Heinze B, Krempl CD, Collins PL.
433 Deletion of nonstructural proteins NS1 and NS2 from pneumonia virus of mice
434 attenuates viral replication and reduces pulmonary cytokine expression and
435 disease. J Virol 2009;83(4):1969-80.

436 [28] Heinze B, Frey S, Mordstein M, Schmitt-Graff A, Ehl S, Buchholz UJ et al.
437 Both Nonstructural Proteins NS1 and NS2 of Pneumonia Virus of Mice are
438 Inhibitors of the Interferon Type I and Type III Responses In Vivo. J Virol
439 2011;85(9):4071-84.

440 [29] Rosenberg HF, Domachowske JB. Pneumonia virus of mice: severe
441 respiratory infection in a natural host. Immunol Lett 2008;118(1):6-12.

442 [30] Claassen EA, van der Kant PA, Rychnavska ZS, van Bleek GM, Easton AJ,
443 van der Most RG. Activation and inactivation of antiviral CD8 T cell responses
444 during murine pneumovirus infection. J Immunol 2005;175(10):6597-604.

445 [31] Frey S, Krempl CD, Schmitt-Graff A, Ehl S. Role of T cells in virus control and
446 disease after infection with pneumonia virus of mice. J Virol 2008;82(23):11619-
447 27.

448 [32] Kruijsen D, Schijf MA, Lukens MV, van Uden NO, Kimpen JL, Coenjaerts FE
449 et al. Local innate and adaptive immune responses regulate inflammatory cell

450 influx into the lungs after vaccination with formalin inactivated RSV. Vaccine 2011;
451 29(15):2730-2741.

452 [33] Polakos NK, Klein I, Richter MV, Zaiss DM, Giannandrea M, Crispe IN et al.
453 Early intrahepatic accumulation of CD8+ T cells provides a source of effectors for
454 nonhepatic immune responses. J Immunol 2007;179(1):201-10.

455 [34] Zaiss DM, de Graaf N, Sijts AJ. The proteasome immunosubunit multicatalytic
456 endopeptidase complex-like 1 is a T-cell-intrinsic factor influencing homeostatic
457 expansion. Infect Immun 2008;76(3):1207-13.

458 [35] Garvey TL, Dyer KD, Ellis JA, Bonville CA, Foster B, Prussin C et al.
459 Inflammatory responses to pneumovirus infection in IFN-alpha beta R gene-
460 deleted mice. J Immunol 2005;175(7):4735-44.

461 [36] Chen W, Anton LC, Bennink JR, Yewdell JW. Dissecting the multifactorial
462 causes of immunodominance in class I-restricted T cell responses to viruses.
463 Immunity 2000;12(1):83-93.

464 [37] Chang J, Braciale TJ. Respiratory syncytial virus infection suppresses lung
465 CD8+ T-cell effector activity and peripheral CD8+ T-cell memory in the respiratory
466 tract. Nat Med 2002;8(1):54-60.

467 [38] Sherman LA, Burke TA, Biggs JA. Extracellular processing of peptide
468 antigens that bind class I major histocompatibility molecules. J Exp Med
469 1992;175(5):1221-6.

470 [39] Kulkarni AB, Morse HC,3rd, Bennink JR, Yewdell JW, Murphy BR.
471 Immunization of mice with vaccinia virus-M2 recombinant induces epitope-specific

and cross-reactive Kd-restricted CD8+ cytotoxic T cells. J Virol 1993;67(7):4086-92.

[40] Percopo CM, Qiu Z, Phipps S, Foster PS, Domachowske JB, Rosenberg HF. Pulmonary eosinophils and their role in immunopathologic responses to formalin-inactivated pneumonia virus of mice. J Immunol 2009;183(1):604-12.

[41] Claassen EA, van Bleek GM, Rychnavska ZS, de Groot RJ, Hensen EJ, Tijhaar EJ et al. Identification of a CD4 T cell epitope in the pneumonia virus of mice glycoprotein and characterization of its role in protective immunity. Virology 2007;368(1):17-25.

[42] Stevens WW, Kim TS, Pujanauski LM, Hao X, Braciale TJ. Detection and quantitation of eosinophils in the murine respiratory tract by flow cytometry. J Immunol Methods 2007;327(1-2):63-74.

Figure Legends

Fig. 1. $CD8^+$ T-cell kinetics in PVM and influenza-infected mice. BALB/c mice were infected *i.n.* with approximately 25 pfu PVM or $1x10^5$ EID_{50} influenza A/HK-x31 and sacrificed at the indicated days p.i. (A) PVM virus titers in the right lung determined by quantitative RT-PCR and converted to PVM-SH gene copy numbers per lung. The dotted line indicates the detection limit. Results are shown as mean ± SEM with 3 mice per group. (B) Frequency of total $CD8^+$ T-cells as percentage of lymphocytes in the BAL determined by flow cytometry at the indicated days p.i. Results are shown as mean ± SEM with 3 mice per group. (C) Frequencies of virus-specific $CD8^+$ T-cells in the BAL were determined by staining with MHC class I tetramers loaded with $NP_{147-155}$ (influenza tetramer) or $M2_{82-290}$ (hRSV tetramer), and tetramers loaded with unrelated peptides were used to measure background staining. The percentage of virus-specific $CD8^+$ T-cells in the BAL of influenza (left graph) or hRSV (right graph) infected mice ($CD62L^-$ tetramer+) are shown after subtraction of background staining. (D, E) Frequencies of virus-specific $CD8^+$ T-cells in the BAL of PVM infected mice, determined as described in (C) with $P_{261-269}$-peptide loaded MHC class I tetramers. (D) Graph showing the results of individual mice and (E) representative FACS plots (gated on $CD8^+$ cells) show the percentage of PVM tetramer+ (tet^+) or hRSV $tetramer^+$ $CD62L^-$ cells at the indicated days p.i. (F, G) BAL cells from PVM-infected mice were restimulated *ex vivo* for 6h in the presence of monensin with or without $P_{261-269}$ peptide. (F) Corresponding graphs showing the results of individual mice (background frequencies in the absence of peptide are subtracted) and (G), representative FACS plots showing frequencies of $IFN\gamma^+$ $CD8^+$ cells after peptide

restimulation. Data are representative of two independent experiments. BAL of uninfected mice did not contain any cells or detectable viral loads.

Fig. 2. NK cell responses in PVM- compared to influenza-infected mice. BALB/c mice were infected *i.n.* with approximately 25 pfu PVM or $1x10^5$ EID_{50} influenza A/HK-x31 and sacrificed at the indicated days p.i. (A) NK cells ($TCR\beta^-DX5^+$) as percentage of total lymphocytes (left panel) or in absolute numbers (right panel) in the BAL, as determined by flowcytometry. (B) Mean fluorescence intensities (MFI) of CD69 expression on NK cells in the BAL. (C) Percentage of IFNγ producing NK cells in the BAL after *ex vivo* restimulation with YAC cells (1:1) in the presence of monensin for 6h. (D) Mice were infected with 150 EID_{50} influenza PR8, 25 pfu PVM (normal dose) or 1250 pfu PVM (high dose) and absolute numbers of NK cells ($DX5^+NKp46^+TCR\beta^-$) in the BAL were determined. Results are shown as mean ± SEM for 3 mice per group. n.d., not determined.

Fig. 3. Effects of DCp immunization on control of PVM infection. Mice were immunized *i.v.* with 5×10^6 $P_{261-269}$-loaded BM-DCs or left untreated, and infected *i.n.* with approximately 15 pfu PVM 3-5 weeks later. 4-5 mice per group were sacrificed on d. 8 and 14 after PVM infection. (A, B) Frequency of $P_{261-269}$-specific $CD8^+$ cells in the BAL at d. 14 p.i. determined by tetramer staining as described in the legend to Fig. 2. (A) Representative FACS plots (gated on $CD8^+$ cells), and (B) corresponding graphs showing results for individual mice. (C) Body weight of individual mice as a percentage of their initial weight. (D) Total numbers of cells in the BAL at d. 8 p.i. (E) Virus titer in the right lung determined by quantitative RT-

PCR and converted to PVM-SH gene copy numbers. Data are representative of two independent experiments. Statistical analysis was performed using a Mann-Whitney U-test. *, $p<0.05$

Fig. 4. Cytokine production and eosinophils in the airways of PVM-infected, DCp-compared to FI-PVM-immunized mice. 4-5 mice per group were immunized *i.v.* with 5 x 10^6 $P_{261-269}$-loaded BM-DCs, or *s.c.* with FI-PVM, and infected *i.n.* with approximately 15 pfu PVM 3-5 weeks later. (A) Relative expression of IFNγ (upper graph) or IL-4 (lower graph) mRNA in the lungs 5 days after PVM infection, determined by Q RT-PCR. (B) Levels of IFNγ (upper graph)and IL-4 (lower graph) in the BAL fluid on d. 5 p.i., determined by luminex. (C) FACS plots showing an example of CD11c and Siglec-F staining on BAL cells of immunized mice 14 days after PVM infection. Gated samples were eosinophils ($CD11c^-Siglec\text{-}F^+$) as described [42]. (D) Frequency of eosinophils in the BAL of individual immunized mice 14 days after PVM infection, determined by flow cytometry. Statistical analysis was performed using a Mann-Whitney U-test. *, $p<0.05$

Fig. 5. Effects of $CD8^+$ T-cell transfer on PVM infection. $CD8^+$ T-cells enriched from pooled lung-, spleen- and MLN-cells of PVM-infected (d. 14 p.i.) or naïve donor mice were transferred *i.v.* into recipient mice that were subsequently infected with approximately 25 pfu PVM and sacrificed at d. 7 p.i. (A) Representative FACS plots of gated $CD8^+$ cells showing $P_{261-269}$-specific T cells ($CD62L^-$PVM tet^+) in the lungs of mice that received $CD8^+$ T-cells of PVM-infected (right) or naïve (left) donors. (B) Frequencies of $P_{261-269}$-specific $CD8^+$ cells in the

562 lungs, determined by tetramer staining. (C) Body weight of individual mice as
563 percentage of their initial weight at the indicated days p.i. (D) Virus titer in the right
564 lung determined by Q RT-PCR and converted to PVM-SH copy numbers.
565 Statistical analysis was performed using a Mann-Whitney U-test. *, $p<0.05$
566

567

Figure 1

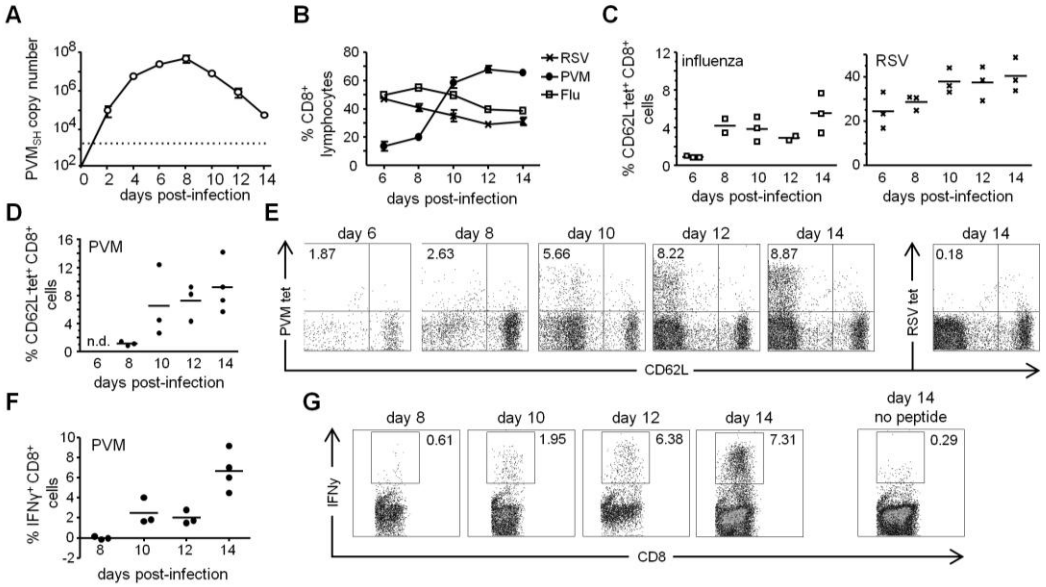

568
569

570

Figure 2

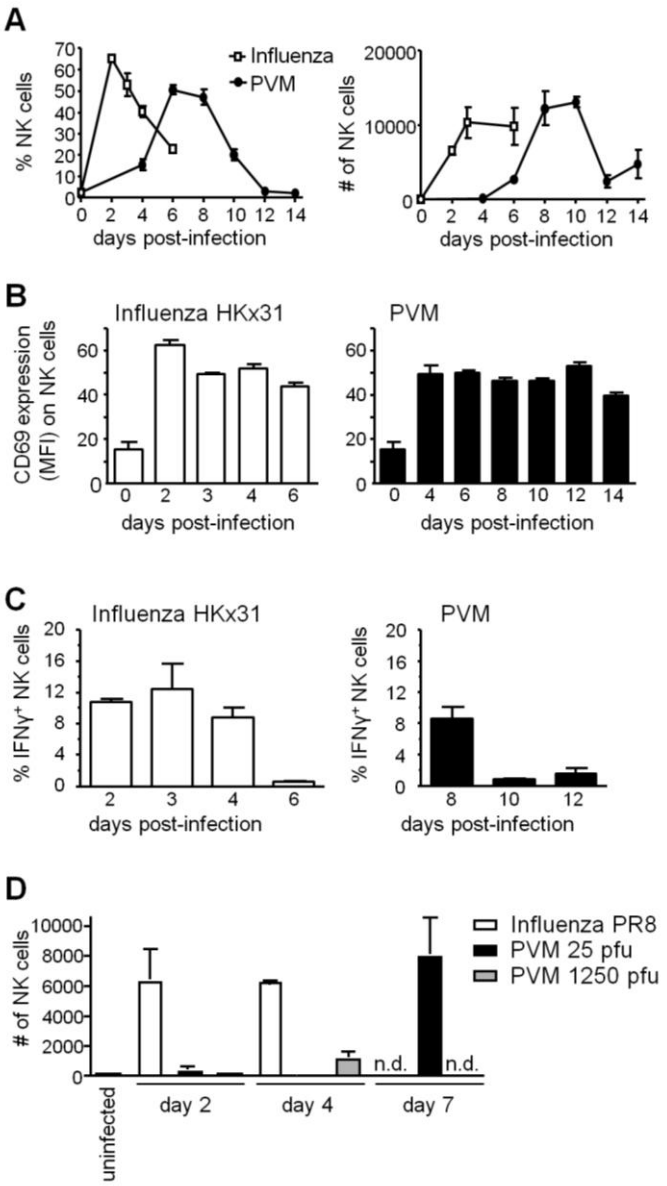

571
572

573

Figure 3

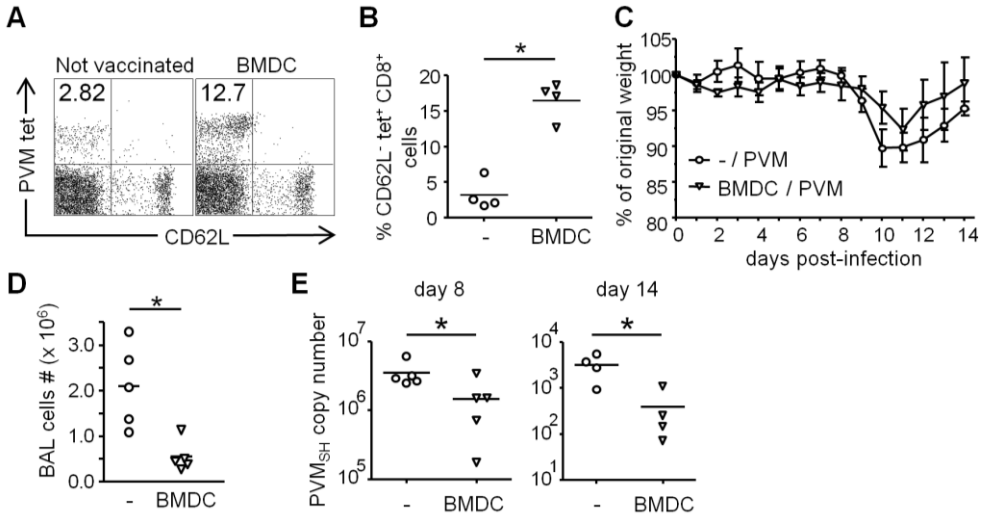

574
575
576

577

Figure 4

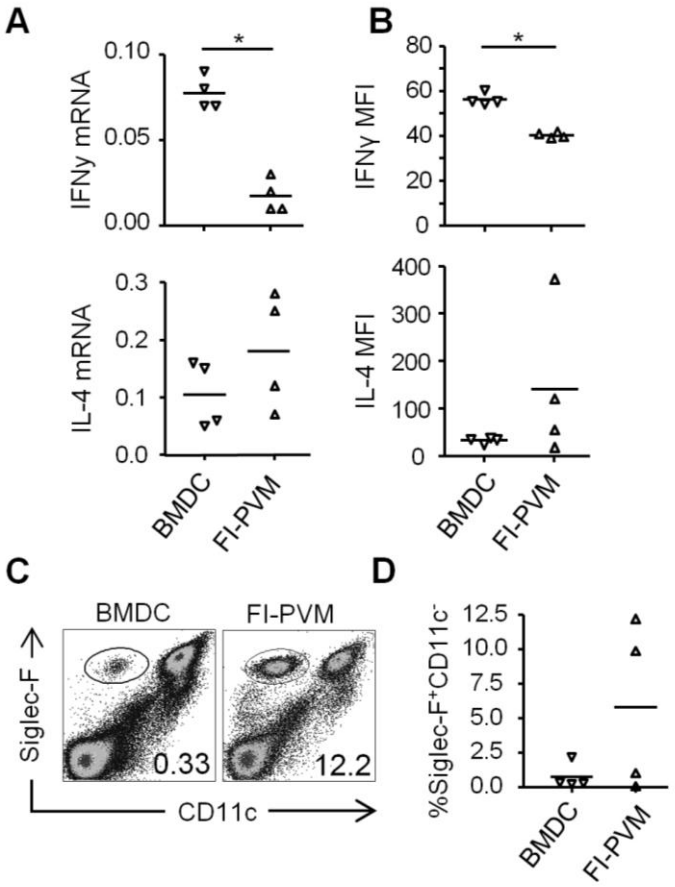

578
579

580

Figure 5

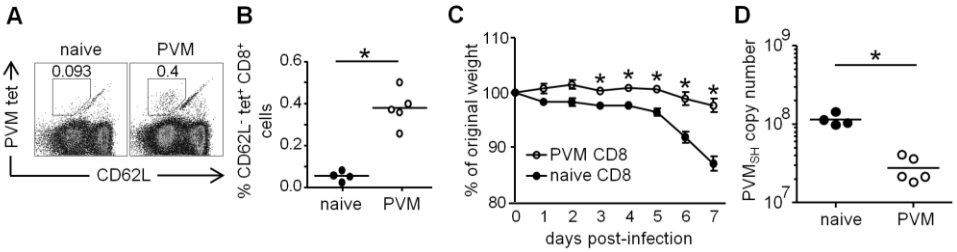

581